

Petro-geochemistry and zircon U-Pb dating of the late Variscan Flamanville granodiorite and its Paleoproterozoic basement (Normandy, France)

Pétrogéochimie et datation U-Pb sur zircon de la granodiorite tardi-varisque de Flamanville et son soubassement paléoprotérozoïque (Normandie, France)

Martin Erwan^{1*},
François Camille²,
Paquette Jean-Louis³,
Capdevila Ramon⁴,
Lejeune Anne-Marie¹

Géologie de la France, n° 1, 2018, p. 34-48, 13 fig., 1 tab. 3 app.

Keywords: Flamanville granodiorite, Armorican Massif, zircon dating, magma genesis, Variscan geology

Mots-clés : Granodiorite de Flamanville, massif Armoricain, datations sur zircon, genèse des magmas, géologie Varisque

Abstract

We report for the first time the petro-geochemical study and the emplacement age of the Flamanville granitoid pluton, which is one of the most pedagogical and frequently visited granitoid in France. This study shows that it consists of a potassic alkaline to calc-alkaline and metaluminous granodiorite with biotite, hornblende and pluri-centimetric potassic feldspar megacrysts. *In situ* U-Pb dating on zircon crystals established that this pluton was formed at 318.1 ± 1.5 Ma, which is older than previously obtained by Rb-Sr and K-Ar methods on biotite (between 299 and 316 Ma). We also report the oldest age measured in France, 2043 ± 4 Ma from *in situ* U-Pb dating on zircon crystals from the Anse du Cul-Rond gneiss, which could be representative of the Paleoproterozoic crust in which the Flamanville pluton emplaced. These zircons also record an age of 547 ± 15 Ma corresponding to metamorphism during the Cadomian orogeny.

Emplaced in a Paleoproterozoic basement affected by the Cadomian orogeny, the Flamanville granodiorite is clearly linked to the Type 2 and Type 3 Variscan metaluminous granitoids from Armorican Massif (Mg- and Fe-KCG, respectively). Major and trace elements, Sr- Nd- and O-isotopic compositions as well as the lack of inherited zircon cores, clearly indicate that the magmatic source is mantellic with only modest crustal influence. This can be

due to mantle metasomatism by crustal fluids/melts during the subduction of the continental crust at the first stage of the collision or to crustal contamination/assimilation during the emplacement of the mantellic magma into the crust.

Résumé

Nous reportons pour la première fois une étude pétrologique, géochimique et géochronologique du pluton de granitoïde de Flamanville, qui est le pluton le plus visité et le plus pédagogique en France. Cette étude montre qu'il a une composition de granodiorite potassique alcaline à calco-alkaline et métalumineuse avec de la biotite, de la hornblende et des mégacristaux pluri-centimétriques de feldspath potassique. Des datations *in situ* U-Pb sur zircons ont été menées et montrent que ce pluton s'est mis en place à 318.1 ± 1.5 Ma, ce qui est plus ancien que les résultats obtenus par de précédentes datations par les méthodes Rb-Sr et K-Ar sur biotite (entre 299 et 316 Ma). Nous reportons également le plus vieil âge mesuré en France, c'est-à-dire 2043 ± 4 Ma obtenu à partir de datations U-Pb *in situ* sur des zircons du gneiss de l'Anse du Cul-Rond, qui pourrait représenter la croûte Paléoprotérozoïque dans laquelle le pluton de Flamanville s'est mis en place. Ces zircons enregistrent également un âge de 547 ± 15 Ma correspondant au métamorphisme lors de l'orogène Cadomien.

Mise en place dans un socle Paléoprotérozoïque affecté par l'orogenèse cadomienne, la granodiorite de Flamanville est clairement liée aux granitoïdes métalumineux varisques de Type 2 et Type 3 du Massif Armoricain (Mg- et Fe-KCG respectivement). Les compositions en éléments majeurs, traces et en isotopes de

¹, Sorbonne Université, CNRS-INSU, Institut des Sciences de la Terre Paris, ISTE-P UMR 7193, F-75005 Paris, France.

², Early Life Traces & Evolution-Astrobiology, Department of Geology, University of Liège, 4000 Liège, Belgium

³, Laboratoire Magmas et Volcans (CNRS UMR 6524), Université Clermont Auvergne; F-63 000 Clermont-Ferrand Cedex, France

⁴, Géosciences Rennes (CNRS UMR6118), Université de Rennes 1, 35042 Rennes, France

*Corresponding author: erwan.martin@sorbonne-universite.fr

Manuscrit reçu le 2 juillet 2018, accepté le 5 novembre 2018

l'O, du Sr et du Nd aussi bien que l'absence de coeurs hérités dans les zircons indiquent clairement que la source magmatique est mantellique avec une faible influence crustale. Cela peut être dû à la métasomatose de la source mantellique par des fluides/magmas crustaux durant la subduction de la croûte continentale au premier stade de la collision ou dû à une contamination/assimilation crustale durant l'emplacement du magma mantellique dans la croûte.

1. Introduction

The Flamanville pluton is probably the most visited intrusive granitoid in France as it is very accessible and pedagogical with its spectacular shape in the landscape as well as its contact with the country rocks, illustrating perfectly well how plutons form (Brun *et al.*, 1990). It has been indirectly characterized as being similar in composition and age to granitoids from the North of the Armorican Massif (AM) such as Ploumanac'h, Albert-Ildut, Saint Renan, Morlaix's Bay, Barfleur and Porzpaol (Ouessant Island) plutons (e.g. Capdevila 2010). However, only three major element analyses on whole rock as well as one K-Ar and three Rb-Sr radiometric analyses on biotite crystals giving ages between 299 and 316 Ma have been published on the Flamanville pluton (Graindor and Wasserburg, 1962; Adams, 1976; Vidal, 1980; Capdevila, 2010; Thiéblemont *et al.*, 2017). Therefore, doubts remain on its place and role in the AM geological history.

In this paper, after a petro-geochemical description we present a new and precise *in situ* U-Pb dating on zircon crystals from the Flamanville pluton. We also report precise U-Pb zircon ages on the gneiss from the Anse du Cul-Rond that could be considered as representative of the oldest crustal basement in which the Flamanville pluton was intruded. Furthermore, this gneiss recorded the oldest stage of the French geological history from the Paleoproterozoic (2.04 Ga) to the Neoproterozoic (547 Ma).

2. Geological background

The AM, a part of the Variscan chain, can be divided into six different domains, the Léon Domain in the North-West, the North Armoricain Domain, the central Armoricain Domain, the South Armoricain Domain and the Lanvaux and Mauges Domains between the last two (Fig. 1; Ballèvre *et al.*, 2013; Ballèvre, 2016 and references therein). It is noteworthy that another subdivision considering only three domains separated by ophiolitic suture zones has been also proposed by M. Faure *et al.* (2005).

The gneiss from l'Anse du Cul-Rond, which could be considered as representative of the crust in which the Flamanville pluton was intruded, is located in the North Armoricain domain (Fig. 1) and was dated both by single and multi-grain ID-TIMS U-Pb zircon method and SHRIMP *in situ* dating in a previous study (Inglis *et al.*, 2004). In this previous study, zircons dated by ID-TIMS were discordant and define a Concordia line intersecting the Concordia at 2061 ± 2.7 Ma, whereas SHRIMP mean $^{207}\text{Pb}/^{206}\text{Pb}$ age on

spot analysis of two grains was 2043 ± 6 Ma. These ages were considered as representative of the crystallization age of the granitic protolith of this rock. U-Pb dating determined from three spot analyses of the zircon overgrowths yielded concordant Neoproterozoic dates at 616.9 ± 6.7 Ma ($\text{MSWD}_{\text{C+E}} = 0.48$; recalculated using Isoplot at the 2σ level) corresponding to the Cadomian metamorphism that affected the zircon crystals (Inglis *et al.*, 2004).

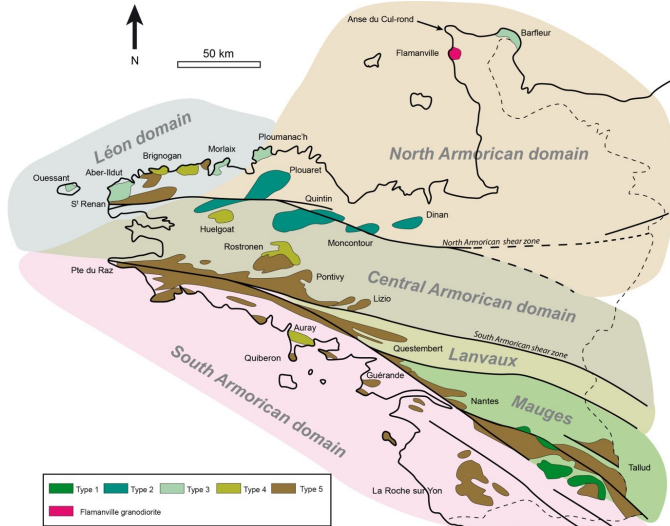


Fig. 1. Location of the five different types of Variscan granitoids in the Armoricain Massif (modified from R. Capdevila 2010). The different domains are from M. Ballèvre *et al.* (2013 and references therein). Type 1: ACG; Type 2: Mg-KCG; Type 3: Fe-KCG; Type 4: CPG; Type 5: MPG. (ACG: calc-alkaline granitoids; Mg-KCG: magnesian calc-alkaline granitoids; Fe-KCG: ferriferous calc-alkaline granitoids; CPG: cordierite-bearing peraluminous granitoids; MPG: muscovite-bearing peraluminous granitoids).

Fig. 1. Localisation des cinq différents types de granitoides varisques dans le Massif armoricain (modifié d'après R. Capdevila, 2010). Les différents domaines proviennent de M. Ballèvre *et al.* (2013). Type 1: ACG; Type 2: Mg-KCG ; Type 3: Fe-KCG ; Type 4: CPG ; Type 5: MPG. (ACG: granitoides calco-alcalins ; Mg-KCG: granitoides calco-alcalins riches en magnésium; Fe-KCG: granitoides calco-alcalins riche en fer ; CPG: granitoides peraluminieux à cordierite; MPG: granitoides peraluminieux à muscovite).

The Flamanville pluton, located in the North Armoricain Domain, was emplaced into Cambrian to Devonian sediments and shows a spectacular contact metamorphism aureole (Fig. 2; e.g. Abréal, 2009 ; Marcoux *et al.*, 2012 and references therein). Based on 4 biotite crystal analyses, it was previously dated between 299 and 316 Ma (Adams, 1976; Vidal, 1980). Despite the imprecise dating, the Flamanville pluton is clearly linked to the Variscan history of the AM.

Variscan granitoids are present in all different Armoricain domains. As suggested by R. Capdevila (2010) and based on petro-geochemical criteria, they can be classified into 5 different types.

- **Type 1:** Calc-alkaline granitoids (ACG; Barbarin, 1999) with biotite and hornblende (Fig. 1). This type is only represented in Vendée (SE of the South Armoricain Shear Zones). Its age is estimated to be around 370-375 Ma, based on U-Pb dating on zircon from the quartzdiorite from Le Tallud of $373 +6-11$ Ma (Cuney *et al.*, 1993).

- **Type 2:** High-K-Mg calc-alkaline granitoids (magnesian KCG; Barbarin, 1999) that consists mainly of metaluminous monzogranites containing biotite and hornblende (Fig. 1). Located along the North Armoricain Shear Zone, they were dated between 329 ± 5 Ma and 291 ± 9 Ma based on Rb-Sr on whole rock dating at Plouaret

and Quintin respectively (Peucat et al., 1984). Unfortunately, no precise U-Pb dating on zircon exists so far for this type of granitoids.

- **Type 3:** High-K-Fe calc-alkaline granitoids (ferriferous KCG; Barbarin, 1999), including metaluminous monzogranite and syenite with biotite and hornblende (Fig. 1). Located in the North of the AM, following a SW-NE Cadomian direction, they were dated between 300 and 310 Ma, based on U-Pb dating on zircon from the Albert Ildut (303.8 ± 0.9 Ma; Caroff et al., 2015) and Ploumanac'h (between 308.8 ± 2.5 and 301.3 ± 1.7 ; Dubois, 2014) massifs.

- **Type 4:** Cordierite-bearing peraluminous granitoids (CPG; Barbarin, 1999) with mostly monzogranites to granites containing biotite and cordierite. Located in the West of the AM, they were dated from 310 to 320 Ma, based on U-Pb dating on zircon at Huelgoat (314 Ma; Ballouard, 2016), Pontivy-Rostrenen (316 ± 3 Ma, Euzen, 1993; 315.2 ± 2.9 Ma, Ballouard et al., 2017).

- **Type 5:** Muscovite-bearing peraluminous granitoids (MPG; Barbarin, 1999), which consist of muscovite-biotite granites. Located all along the South Armorican Shear Zone and in the Léon Domain they were dated between 310 and 320 Ma, based on U-Pb dating on zircon and monazite from the Guérande: 309.7 ± 1.3 Ma (Ballouard et al., 2015), Lizio: 316 ± 5.6 Ma (Tartèse et al., 2011a), Questembert: 316 ± 2.9 Ma (Tartèse et al., 2011b) and Saint Renan: 316 ± 2.0

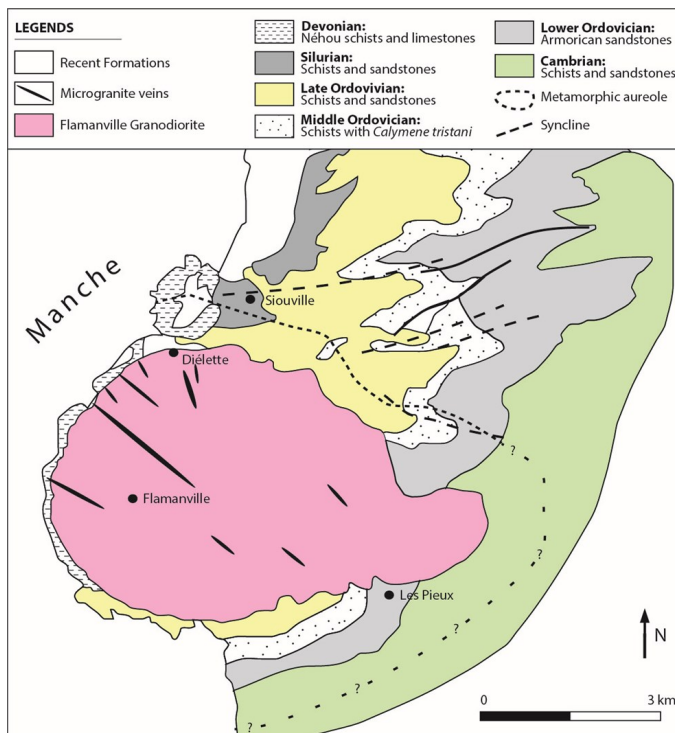


Fig. 2. Geological map of the Flamanville pluton and its metamorphism aureole (contoured by the dotted black line). The pluton was emplaced into Cambrian to Devonian sediments that consist mainly of arkose, pelite and sandstone. Modified from E. Marcoux et al. (2012). Samples from this study were collected close to Diélette (see the text for further information).

Fig. 2. Carte géologique du pluton de Flamanville et son auréole de métamorphisme (représentée par la ligne noire en pointillés). Le pluton s'est mis en place dans des sédiments cambriens à dévonien composés principalement d'arkose, de pélite et de grès. Modifiée après E. Marcoux et al. (2012). Les échantillons de cette étude ont été collectés à proximité de Diélette (voir le texte pour la localisation précise).

Ma (Le Gall et al., 2014) massifs

3. Petrographical characteristics

Samples from this study were collected at Diélette (at the entrance of the nuclear power plant; N $49^{\circ}32'49.13''$ W $1^{\circ}52'13.37''$; Figs. 2 and 3a), where thousands of students and tourists come every year to observe and study the pluton and its metamorphic aureole. Fresh samples were collected from the pluton rim at 20-40 m from the sharp contact with the country rocks that consist of a spectacular garnetite formed by contact metamorphism (Abréal, 2009). The whole rock is a granitoid containing pluri-millimetric and xenomorphic quartz crystals, automorphic feldspars, and sub-millimetric ferro-magnesian minerals (biotite and amphibole; Fig. 3). In addition, pluri-centimetric pale pink orthoclase crystals (usually zoned (Rapakivi texture); Fig. 3d) are present and clearly visible on the outcrop. Rounded enclaves rich in ferro-magnesian minerals are present in this location (Figs. 3b and c). However, unlike in the southern contact of the pluton (Le Havre Jouan in the North of the Sciotot Bay), no sharp enclaves of metamorphosed country rocks are observed. At the sampling location, centimeter-thick aplite veins are also present and overprint all the features described above (Fig. 3) and are clearly linked to the late history of the pluton emplacement and cooling.

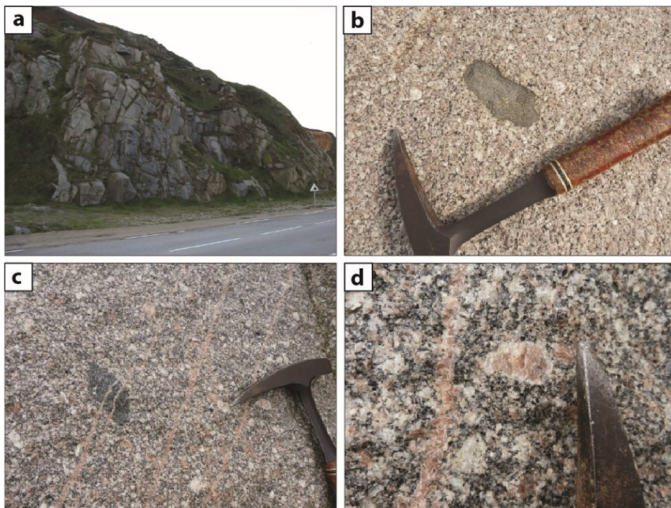


Fig. 3. Photos (a) de l'affleurement où les échantillons ont été collectés à Diélette (France), (b) d'une enclave ferromagnésienne dans la granodiorite porphyrique ; (c) des veines d'aplite recoupant la granodiorite et les enclaves ; (d) d'un phénocrystal de feldspath zoné à texture Rapakivi.

Fig. 3. Photos (a) de l'affleurement où les échantillons ont été collectés à Diélette (France), (b) d'une enclave ferromagnésienne dans la granodiorite porphyrique ; (c) des veines d'aplite recoupant la granodiorite et les enclaves ; (d) d'un phénocrystal de feldspath zoné à texture Rapakivi.

The Flamanville granitoid has a porphyritic texture (Figs. 3 and 4) with pluri-centimetric potassic feldspar megacrysts and a pluri-millimetric matrix composed at more than 90% of quartz (20-25%), plagioclase that is mostly albitic (45-50%; An₅₋₃₀Ab₆₇₋₉₅Or₀₋₈; Fig. 5b and Appendix 1) and potassic feldspar (25-30%; An₀Ab₇₋₂₅Or₇₄₋₉₃; Fig. 5b and Appendix 1) and some ($\leq 10\%$) biotite (Al-poor biotite with $0.55 < X_{Mg} < 0.65$ and $2.78 < Si < 2.9$; Fig. 5a and Appendix 1), green amphibole (Edenite: Na+K>0.05 and X_{Mg}<0.5; Fig. 5c and Appendix 1) and accessory minerals (<1%) such as titanite, apatite, magnetite, monazite and zircon.

The presence of Al-poor biotite and amphibole, and the absence of cordierite ($Al_3Mg_2AlSi_5O_{18}$) and muscovite (KAl_2

$(\text{AlSi}_3\text{O}_{10})(\text{OH},\text{F})_2$) suggest a metaluminous affinity like the Type 1, 2 and 3 Variscan granitoids from the Armorican Massif described above.

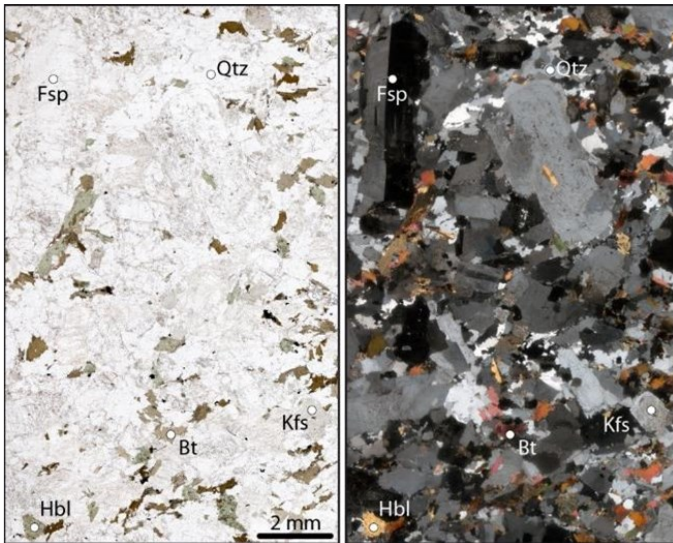


Fig. 4. Major phases of the Flamanville granodiorite. On the left observation under plane polarized light and on the right under cross-polarized light (Qtz: quartz; Fsp: feldspar; Kfs: potassic feldspar; Bt: biotite; Hbl: Hornblende).

Fig. 4. Phases majeures de la granodiorite de Flamanville. A gauche, observation en lumière polarisée non-analysée et à droite, lumière polarisée analysée (Qtz : quart z; Fsp : feldspath ; Kfs : feldspath potassique ; Bt : biotite; Hbl : Hornblende).

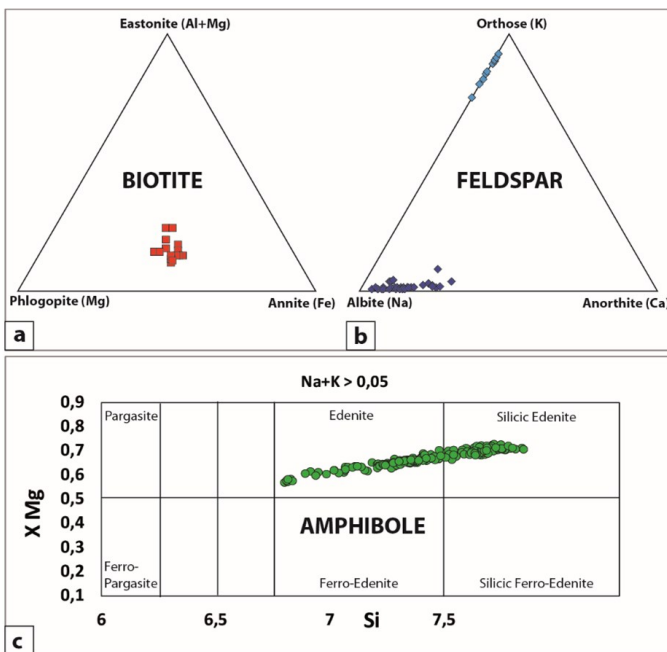


Fig. 5. Composition diagrams of (a) biotite, (b) feldspar and (c) amphibole crystals from the Flamanville pluton.

Fig. 5. Diagrammes de composition de cristaux de (a) biotites, (b) feldspaths et (c) amphibiols provenant du pluton de Flamanville.

4. Geochemistry

4.1. Analytical methods

Whole rock samples were crushed into powder for bulk major, trace and Sr-Nd isotopic analyses. Zircon crystals were extracted from the whole rock by heavy liquid (methylene iodide) methods for Laser-Ablation Inductively-Coupled Plasma Mass-Spectrometry (LA-ICPMS) U-Pb dating and oxygen isotope ratio determination. Major and trace element concentration measurements were performed

in the SARM (Nancy, France) and listed in Table 1. U-Th-Pb isotopic data on zircons were obtained at the Laboratoire Magmas & Volcans (France) by LA-ICPMS. The analyses involved the ablation of minerals with a Resonetics M-50 laser system operating at a wavelength of 193 nm. Spot diameters of 20 μm were associated to repetition rates of 3 Hz and fluency of 2.5 J/cm². The ablated material was carried in helium and then mixed with nitrogen and argon before injection into the plasma source of a Thermo Element XR Sector Field high-resolution ICP-MS. The analytical method for isotope dating with LA-ICPMS is similar to that reported in previous studies (Hurai *et al.*, 2010; Paquette *et al.*, 2014; Mullen *et al.*, 2018). Data are corrected for U-Pb fractionation during laser sampling and for instrumental mass bias by standard bracketing with repeated measurements of the GJ-1 zircon standard (Jackson *et al.*, 2004). The reproducibility and accuracy of the corrections were controlled by repeated analyses of the 91500 zircon standard (Wiedenbeck *et al.*, 1995) treated as unknown. Data reduction was carried out with the GLITTER® software package (Van Achterbergh *et al.*, 2001). The calculated ratios were exported and Concordia ages and diagrams were generated using Isoplot/Ex v. 2.49 software package (Ludwig, 2001). The concentrations of U, Th and Pb were calibrated relative to the certified contents of the GJ-1 zircon standard (Jackson *et al.*, 2004). In the case of the Variscan granite, the zircon analytical results were projected on $^{207}\text{Pb}/^{206}\text{Pb}$ versus $^{238}\text{U}/^{206}\text{Pb}$ diagrams (Tera and Wasserburg, 1972), where the analytical points plot along a mixing line between the common Pb composition at the upper intercept and the zircon age at the lower intercept. This method is commonly used to date Phanerozoic zircons using *in situ* techniques (Mullen *et al.*, 2018). The analytical data are provided in Table 1. In the text, table and figures, all uncertainties on isotope ratios and ages are quoted at the 2σ level.

Oxygen isotopes were measured by laser fluorination at the stable isotope geochemistry lab at the IPGP (France). Bulk zircon crystals (0.4-1mg) were run between UWG2 standards ($\delta^{18}\text{O}=5.75\text{\textperthousand}$) on which the reproducibility is $<0.1\text{\textperthousand}$.

Strontium and Neodymium isotopic ratios were measured on the whole rocks at the Laboratoire Magmas et Volcans (France). The isotopic ratios were measured on a Thermo-Finnigan Triton mass spectrometer. The reproducibility of the analytical method is ± 0.000012 for $^{87}\text{Sr}/^{86}\text{Sr}$ based on replicates of the NBS987 international standard and ± 0.000006 for $^{143}\text{Nd}/^{144}\text{Nd}$ based on replicates of the JnDi-1 reference material.

4.2. Major and trace elements

As illustrated in Fig. 6, the so-called Flamanville 'granite' is actually a granodiorite (at the limit with monzonodiorite). One of the best ways to compare granitoids from their major element compositions is based on their aluminous and alkaline affinities. The molecular $\text{Al}_2\text{O}_3/\text{SiO}_2$

(CaO+Na₂O+K₂O), known as A/CNK, testifies to metaluminous and peraluminous affinity when <1 and >1 respectively. The molecular Al₂O₃/(Na₂O+K₂O), known as A/NK, reveals peralkaline compositions when <1. The Variscan granitoids from the Armorican Massif show a continuous evolution from Type 1 to Type 5. Indeed, the alkalinity increases (A/NK decreases from 2.2 to 1.5-1) as the composition is evolving from metaluminous to peraluminous (A/CNK increasing from 0.75 to 1.5). The alkalinity and more specifically the aluminous affinity could reflect the importance of a crustal magmatic source as the continental crust, including its pelitic sediment cover, is overall peraluminous due to long-term leaching. Indeed, the long-term erosion and alteration of the continental crust leads overall to a decrease of alkaline element abundances, due to their high solubility in water and to a relative increase in aluminum abundance due to low solubility in water. Therefore, granitoids that show a A/CNK > 1.2 have a dominant crustal origin. As suggested by R. Capdevila (2010) and based on their alkaline index, Type 1, 2 and 3 were generated mainly from mantellic magmatic sources with increasing crustal influence from Type 1 to Type 3, while the Type 4 have both mantellic and crustal magmatic sources and the Type 5 has overwhelmingly a crustal magmatic source.

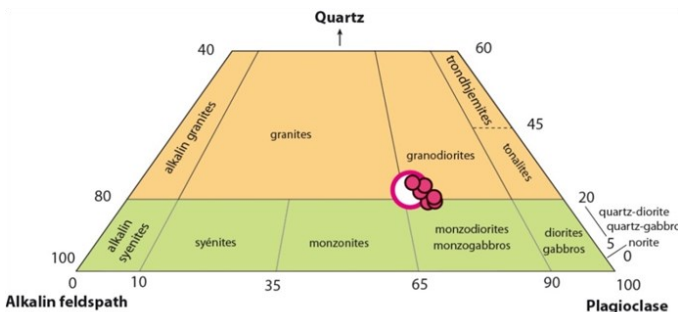


Fig. 6. Flamanville granitoid modal composition (large white circle; determined by point counting technique on 3 different thin sections) and normative compositions (pink circles; data are from this study and Capdevila (2010)) reported in the Streckeisen diagram.

Fig. 6. Composition modale du granitoïde de Flamanville (cercle blanc ; déterminé par comptage de point sur 3 lames minces différentes) et compositions normatives (points roses ; les données proviennent de cette étude et de Capdevila (2010)) reportés dans le diagramme de Streckeisen.

As illustrated by Fig. 7, the Flamanville granodiorite could be attributed to the Type 2 or Type 3 (KCG; Barbarin, 1999). The Mg/(Fe+Mg) from the granodiorite ranges from <0.1 (ferriferous) up to 0.6 (magnesian; and (Fe+Mg+Ti)*1000 <105; this study and Capdevila, 2010) which correspond to both Type 2 and Type 3 respectively. Finally, the Flamanville pluton consists of a potassic alkaline to calc-alkaline and metaluminous granodiorite with biotite and hornblende, like the Type 2 and Type 3 Variscan granitoids defined by R. Capdevila (2010), corresponding to KCG from Barbarin (1999).

The trace element composition (Table 1) illustrated in Fig. 8 is characterized by a relatively smooth but fractionated spidergram with large Nb and Ta anomalies. This could reflect a metasomatized mantle source, which is expected during collisional magmatism as the mantle has been previously metasomatized by subduction fluids. Other granitoids from the Type 3 display similar pattern but

generally with pronounced Ba, Sr and Eu anomalies. These differences could be explained by slightly different magma sources or condition of partial melting but also by different proportion of mineral fractionation during crystallization. While the interpretation of the trace element composition would require further investigation, it is clear in terms of trace element composition that Flamanville and Type 3 granitoids have intermediate composition between Type 1 (mainly mantellic source) and Type 5 (crustal source).

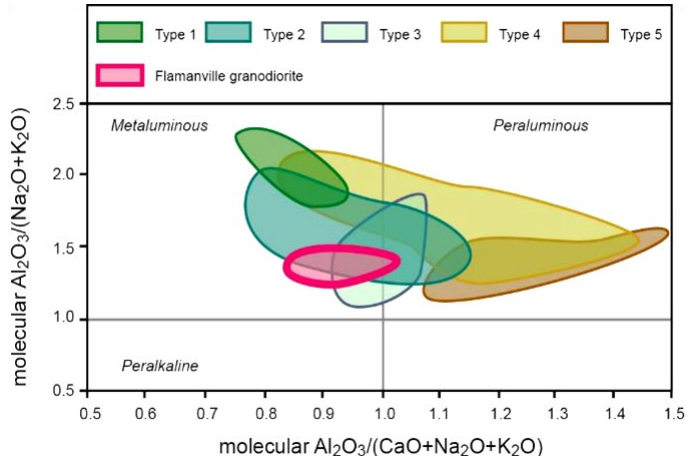


Fig. 7. Flamanville granodiorite compared to the five different types of Variscan granitoids in the Armorican Massif, in respect to their aluminous and alkaline affinities. Dataset are from the R. Capdevila compilation (2010) except for the Flamanville dataset from this study. Type 1: ACG; Type 2: Mg-KCG; Type 3: Fe-KCG; Type 4: CPG; Type 5: MPG.

Fig. 7. La granodiorite de Flamanville comparée aux cinq différents types de granitoides du Massif armoricain en fonction de leurs affinités alumineuses et alcalines. Les données proviennent de la compilation de R. Capdevila (2010) et de cette étude. Type 1: ACG ; Type 2 : Mg-KCG ; Type 3 : Fe-KCG ; Type 4 : CPG ; Type 5 : MPG.

	(Wt.%)
SiO ₂	66,5
Al ₂ O ₃	15,4
Fe ₂ O ₃	3,02
MgO	2,18
CaO	3,19
Na ₂ O	4,45
K ₂ O	3,61
TiO ₂	0,47
P ₂ O ₅	0,20
MnO	0,05
<i>Sum</i>	99,1

	(ppm)
Cs	5,70
Rb	144
Ba	892
Th	28,3
U	7,70
Nb	12,1
Ta	0,90
La	69,3
Ce	121
Pb	11,6
Sr	868
Nd	40,3
Sm	5,40
Zr	250
Hf	6,60
Eu	1,34
Gd	3,74
Tb	0,45
Dy	2,17
Y	10,0
Ho	0,40
Er	0,98
Yb	0,98
Lu	0,15

Table 1. Major and trace element composition of the Flamanville granodiorite from this study. The location of the analyzed sample is indicated in Fig. 2.

Tableau 1. Composition en éléments majeurs et traces de la granodiorite de Flamanville de cette étude. La localisation de l'échantillon analysé est indiquée sur la Fig. 2.

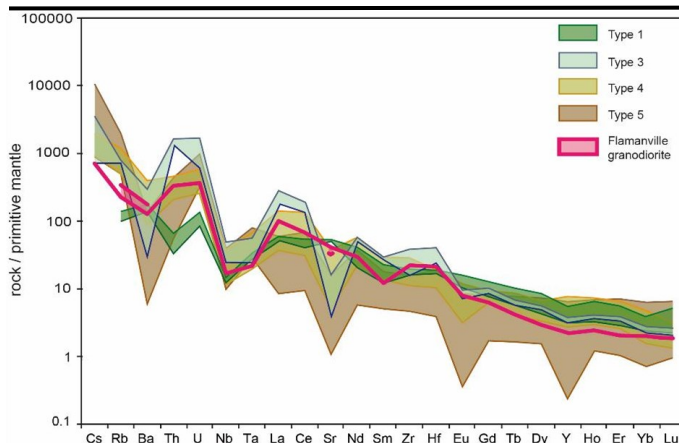


Fig. 8. Flamanville granodiorite comparison with the other types of Variscan granitoids from the Armorican Massif (no data are available for Type 2) in respect to trace elements. Dataset are from the R. Capdevila compilation (2010) except for the Flamanville dataset (this study). The primitive mantle normalization is based on values from S.S. Sun and W.F. McDonough (1989). Type 1: ACG; Type 2: Mg-KCG; Type 3: Fe-KCG; Type 4: CPG; Type 5: MPG.

Fig. 8. Comparaison des éléments traces de la granodiorite de Flamanville et des autres types de granitoids Variscains du Massif Armorican (pas de données existantes pour le Type 2). Les données proviennent de la compilation de R. Capdevila (2010) et de cette étude. La normalisation au manteau primitif est basée sur les valeurs de S.S. Sun and W.F. McDonough (1989). Type 1 : ACG ; Type 2 : Mg-KCG ; Type 3 : Fe-KCG ; Type 4 : CPG ; Type 5 : MPG.

4.3. Isotopic composition

Oxygen isotope ratios on zircon crystals from the Flamanville granodiorite were measured and led to a $\delta^{18}\text{O} = 5.79 \pm 0.25\text{\textperthousand}$. It is noteworthy that the $0.25\text{\textperthousand}$ reproducibility is higher than what is measured on silicate standards ($<0.1\text{\textperthousand}$), which could be explained by the low amount of zircon analysed (as low as 0.4 mg for one analysis) and possibly a relatively heterogeneous composition in a single crystal and between them. *In situ* O-isotopes measurement should be the next step in determining the detailed composition of zircon crystals in the Flamanville pluton.

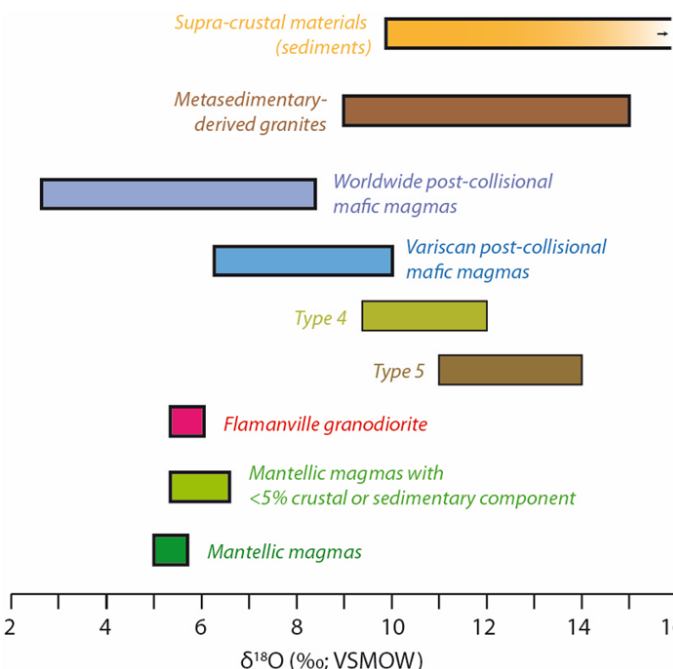


Fig. 9. Oxygen isotopic composition of zircon crystals from Flamanville granodiorite compared to different origin of zircon crystals (values are from O'Neil and Chappell, 1977; Eiler, 2001; Cavosie *et al.*, 2005; Bindeman, 2008; Couzinié *et al.*, 2016). Type 4 and 5 are from whole rock analyses (Euzen, 1993).

Fig. 9. Composition des isotopes de l'oxygène de cristaux de zircons provenant de la granodiorite de Flamanville comparée à différentes origines de cristaux de zircons (valeurs de O'Neil and Chappell, 1977 ; Eiler, 2001 ; Cavosie *et al.*, 2005 ; Bindeman, 2008 ; Couzinié *et al.*, 2016). Les Types 4 et 5 proviennent d'analyses en roche totale (Euzen, 1993).

O-isotope compositions of zircon crystals from pure mantellic magma is expected to be 5.3 ± 0.3 (e.g. Bindeman, 2008 and references therein; Fig. 9). Lower values reflect magmatic sources that have been affected by hydrothermalism at high temperature ($>300^\circ\text{C}$) and higher values reflect high- $\delta^{18}\text{O}$ supracrustal sources such as metasediments or any source that has been affected by hydrothermalism at low temperature ($<300^\circ\text{C}$; Fig. 9). Therefore, the slightly high value of $5.79 \pm 0.25\text{\textperthousand}$ measured in Flamanville granitoid compared to the mantellic value could most likely reflects a dominant mantellic source affected by some modest crustal signature. The high $\delta^{18}\text{O}$ values measured in zircon crystals from post collisional KCG from the French Massif Central are also explained by an interaction between the mantle peridotitic source and subducted crustal material or fluids/melts released from them (Couzinié *et al.*, 2016). It is noteworthy that $\delta^{18}\text{O}$ obtained on whole rock samples from Type 4 and 5 granitoids ($9\text{--}14\text{\textperthousand}$; Euzen, 1993) are in agreement with a crustal origin (partial melting of metasediments).

Age corrected $^{87}\text{Sr}/^{86}\text{Sr}$ and $^{143}\text{Nd}/^{144}\text{Nd}$ initial isotope compositions are 0.70519 and 0.51218, respectively. Hence, the granodiorite has $\epsilon_{\text{Sr}(318\text{Ma})} = +1.47$ and $\epsilon_{\text{Nd}(318\text{Ma})} = -0.97$, indicating isotopic ratios close to the contemporaneous Variscan primitive mantle values, in agreement with a mantellic origin. However, based on Sr- and Nd-isotopes only, it is ambiguous to draw any clear conclusion on the magma source. Indeed, a continental crust that was 1.2–1.5 Ga old during the Variscan history ($\sim 318\text{Ma}$) would have had comparable isotopic values to the mantle and therefore to the initial Flamanville granodiorite and any other Variscan KCG and vaugnerites (mafic magma associated to KCG; Moyen *et al.*, 2017). Therefore, while the Sr- and Nd-isotopes composition is in agreement with a mantellic origin, a crustal influence cannot be ruled out based on these isotopes only.

In addition to major and trace elements, the O- Sr- and Nd-isotopic compositions of the Flamanville granodiorite is in agreement with a mantellic origin, however we cannot rule out any mantle source metasomatism by crustal fluids/melts during the subduction of the continental crust at the first stage of the collision, at least 30 Ma before the partial melting that initiated the formation of the Flamanville granodiorite, or some crustal contamination/assimilation during the mantellic magma emplacement into the crust.

4.4. *In situ* zircon U-Pb dating

4.4.1. Flamanville granodiorite

Zircons from the granodiorite show oscillatory zoning (Fig. 10) and a systematically high Th/U ratio of 0.5 ± 0.2 , that is usually observed in magmatic zircon crystals (Kirkland *et al.*, 2015). The U content may reach high values, up to 1700 ppm and exceptionally for one spot, 7500 ppm and 12800 ppm of U and Th, respectively. Nevertheless, both cathodoluminescence images and U-Pb dating results do not evidence any metamictization of the

zircon grains. The 31 analysed spots yield a lower intercept age of 318.1 ± 1.5 Ma (MSWD= 0.37; Fig. 12; Appendix 2). As mentioned above, the only 4 dating obtained by Rb-Sr and K-Ar on biotite crystals show ages from 299 to 316 Ma. Age inferred from biotite analyses reflects when the pluton reached the temperature of 250–400°C during its cooling (closing temperatures of the Rb-Sr and K-Ar isotopic systems in biotite). Therefore, the high closing temperature of the U-Pb system in zircon makes this dating method the

best estimate of the magma emplacement while the biotite dating gives clue on the magma cooling history. The lack of any inherited zircon core can also be noticed. It implies that crustal melting or assimilation that could lead to zircon crystals incorporation into the magma during its emplacement is limited.

4.4.2. Gneiss from L'Anse du Cul-Rond

Zircon crystals from the gneiss show also a fine oscillatory zoning (Fig. 10) and a Th/U ratio ranging from 0.11 and 0.45 regardless of the amounts of U and Th. Only one spot performed in the grain B05c display a Th/U ratio below 0.01 corresponding to a low Th content. 21 spots provide concordant analyses which yield a Concordia age at 2043.1 ± 3.8 Ma (MSWD 0.96; Fig. 11; Appendix 3) while the whole dataset of 29 analyses allow to calculate a Discordia line with a similar upper intercept age of 2046 ± 5 Ma (Fig. 12). One analysis (Zircon B05c) is discordant at 547 ± 15 Ma. The obtained Paleoproterozoic age of 2043 Ma is interpreted as the crystallisation age for the granite protolith, while the 547 Ma age obtained on a single zircon crystal is comparable to age of the Cadomian metamorphism that affected the whole region (e.g. Chantraine *et al.*, 1988; Le Corre *et al.*, 1991; Ballèvre *et al.*, 2013 for a review). The protolith age is in agreement with the previous SHRIMP ages (Inglis *et al.*, 2004). The Neoproterozoic age reported in our study is significantly younger than that calculated by J.D. Inglis *et al.* (2004) from three zircon tips.

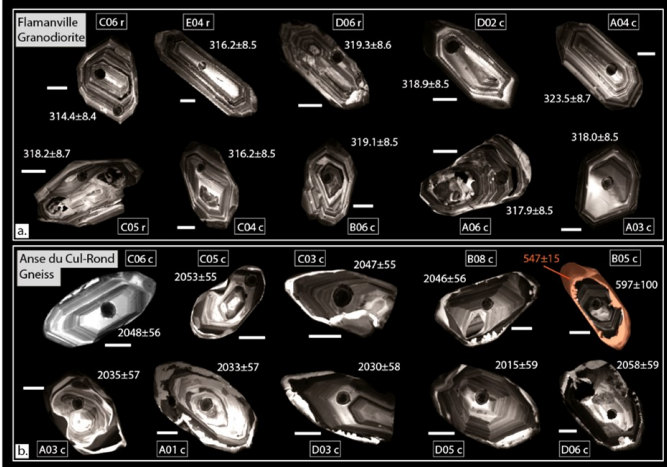


Fig. 10. Cathodoluminescence images of selected zircons from (a) Flamanville Granodiorite and corresponding LA-ICP-MS $^{206}\text{Pb}/^{238}\text{U}$ spot ages in Ma and (b) from l'Anse du Cul-Rond gneiss and corresponding $^{207}\text{Pb}/^{206}\text{Pb}$ ages in Ma. The orange value is the $^{206}\text{Pb}/^{238}\text{U}$ age of the rim of the B05c zircon. Errors are 2σ . White scale bars are 10 µm.

Fig. 10. Images en cathodoluminescence des zircons sélectionnés provenant de (a) la granodiorite de Flamanville et âges $^{206}\text{Pb}/^{238}\text{U}$ obtenus en LA-ICP-MS en Ma et provenant des (b) gneiss de l'Anse du Cul-Rond et âges $^{207}\text{Pb}/^{206}\text{Pb}$ correspondant en Ma. La valeur orange représente l'âge $^{206}\text{Pb}/^{238}\text{U}$ de la bordure externe du zircon B05c. Les erreurs sont données à 2σ . L'échelle blanche représente 10 µm.

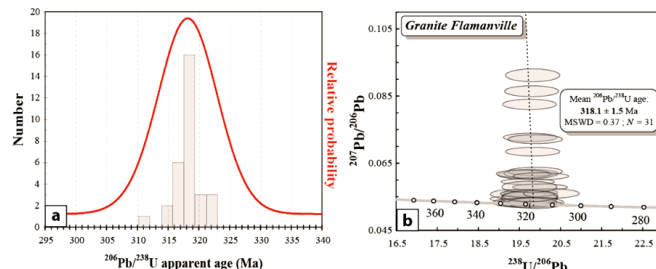


Fig. 11. (a) Age histogram for the granodiorite and (b) corresponding Concordia diagram of F. Tera and G.J. Wasserburg (1972). Error ellipses are 2σ .

Fig. 11. (a) Histogramme des âges de la granodiorite de Flamanville et (b) diagramme Concordia de F. Tera and G.J. Wasserburg (1972) correspondant. Les erreurs sont données à 2σ .

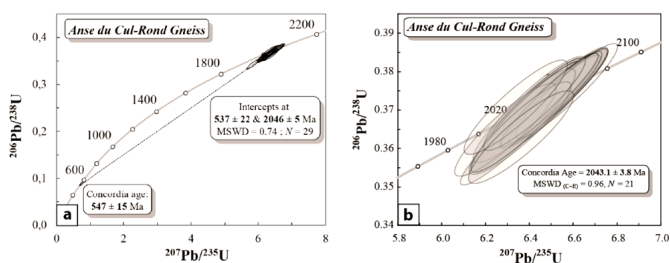


Fig. 12. (a) Concordia diagram for LA-ICP-MS U-Th-Pb analyses on zircons from the gneiss and (b) magnification of (a) for concordant zircons. Error ellipses are 2σ .

Fig. 12. (a) Diagramme Concordia pour les analyses U-Th-Pb sur zircons au LA-ICP-MS provenant des gneiss de l'Anse du Cul-Rond et (b) agrandissement de (a) pour les zircons concordants. Les erreurs sont données à 2σ .

5. The Flamanville granodiorite in the Variscan history of the Armorican Massif

The increase of peraluminous composition from Type 1 (ACG) to Type 5 (MPG) Variscan granitoids could indicate an increase of the role of the continental crust in the Variscan magmatism. As discussed above, the Flamanville granodiorite corresponds to Type 2 and Type 3 (KCG) and seems to have a mantellic origin with a limited crustal signature. If we intend to discuss the origin of magmatism in the AM during the Variscan history, the Type 1 granitoids that are mantellic in origin, were most likely generated by partial melting of the mantle wedge in the pre-Variscan subduction at about 380–370 Ma (Fig. 13). As well illustrated by the Fig. 13, all the granitoids from Types 2, 3, 4 and 5 are contemporaneous (~300–320 Ma) with very different origins from pure crustal to mantellic. The intensification of magmatism between 320 and 300 Ma in the AM could be attributed to a slab break-off at about 350–330 Ma (Ballèvre *et al.*, 2013 and references therein). Indeed a slab break-off leads to an upward asthenospheric flux that can, as a heat source and by inducing an uplift, trigger the lithospheric partial melting. Furthermore, as discussed by Bernard-Griffiths *et al.* (1985) and Ballouard *et al.* (2015), this scenario could also explain the increase of more radiogenic crustal and supracrustal components in the magmatic source of these granitoids from North to South as indicated

by initial Sr and Nd isotope ratios in granitoids along the South Armorican Shear Zone.

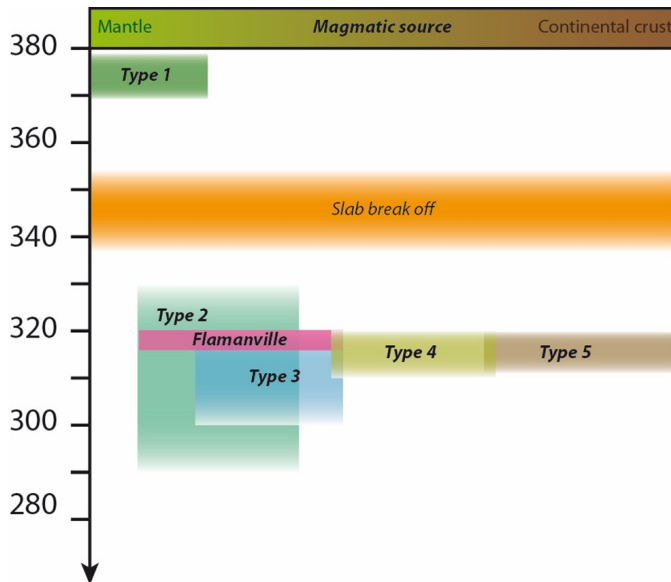


Fig. 13. Evolution of the granitoid magmatic sources during the Variscan orogeny in the Armorican Massif. The slab break-off at about 350–330 Ma is discussed in Ballèvre *et al.* (2013; and references therein). It is noteworthy that Type 1, 3, 4 and 5 have been dated by precise U-Pb dating on zircon while Type 2 has been dated by Rb-Sr method on whole rock, which could explain the wider age range (see text for details). Type 1: ACG; Type 2: Mg-KCG; Type 3: Fe-KCG; Type 4: CPG; Type 5: MPG.

Fig. 13. Évolution des sources magmatiques des granitoïdes durant l'orogenèse varisque dans le Massif armoricain. Le détachement du panneau lithosphérique à environ 350–340 Ma est discuté dans Ballèvre *et al.* (2013 ; et références incluses). Il est important de noter que les Types 1, 3, 4 et 5 ont été datés par des méthodes précises (datations U-Pb sur zircon) alors que les Types 2 ont été datés par la méthode Rb-Sr sur roche totale, ce qui pourrait expliquer la gamme plus large d'âges enregistrée (voir texte pour plus de détails). Type 1: ACG ; Type 2 : Mg-KCG ; Type 3 : Fe-KCG ; Type 4 : CPG ; Type 5 : MPG.

6. Conclusion

The well-known Flamanville ‘granite’ is actually a granodiorite (at the limit with monzodiorite) and was formed at 318.1 ± 1.5 Ma, which is older than previously estimated. The Flamanville granitoid is petro-geochemically close to Variscan Type 2 and Type 3 (KCG) metaluminous granitoids from the Armorican Massif.

Major and trace elements as well as Sr- Nd- and O-isotope compositions tend to indicate that the magmatic source is mantellic with a low crustal influence. This crustal influence could come from mantle metasomatism by crustal fluids/melts during the subduction of the continental crust at the first stage of the collision, at least 30 Ma before the partial melting that initiated the Flamanville granodiorite occurred, or from crustal contamination/assimilation during the mantellic magma emplacement into the crust.

The age of the Flamanville pluton basement was obtained on zircon crystals from the Anse du Cul-Rond gneiss that we dated around 2045 Ma. The same zircon crystals were affected by Cadomian metamorphism at 547 Ma. The lack of inherited zircon cores in Flamanville granodiorite is consistent with a modest crustal influence on its genesis.

Finally, including the Flamanville pluton emplacement, the Variscan magmatism in the AM that mostly took place between 320 and 300 Ma, could have been triggered by a slab break-off at 330–350 Ma. This scenario could explain the intensification of granitoid genesis in the AM as well as

the magmatic source transition from mantellic to crustal from North to South. In order to confirm this, it would be necessary to date precisely zircon crystals from the AM granitoids by *in situ* U-Pb method. This would help to better constrain the chronology of Variscan events in the region and even the French geological history from 2 Ga to 300 Ma.

Acknowledgments

The first author thanks François Baudin for showing him the Flamanville geological site at the first place and Lucy Whiteley for proofreading the manuscript. We are also grateful to Chantal Bosq and Delphine Auclair for Sr and Nd isotopic analyses, Pierre Cartigny for the accessibility to his lab for O-isotopes analyses.

REFERENCES

- Abréal A.** (2009) - L'auréole du granite de Flamanville et ses grenats : métamorphisme de contact. *J. Mineral.*, 111–134.
- Adams C.J.D.** (1976) - Geochronology of the Channel Islands and adjacent French mainland. *J. Geol. Soc.*, 132, p. 233–250. doi: 10.1144/gsjgs.132.3.0233
- Ballèvre M.** (2016) - Une histoire géologique du Massif armoricain. *Géochronique*, 16–46.
- Ballèvre M., Bosse V., Dabard M.-P., Ducassou C., Fourcade S., Paquette J.-L., Peucat, J.-J., Pitra P.** (2013) - Histoire Géologique du massif Armorican : Actualité de la recherche. *Bulletin de la Société Géologique et Minéralogique de Bretagne*, Soc, 5–96.
- Ballouard C.** (2016) - Origine, évolution et exhumation des leucogranites peralumineux de la chaîne hercynienne armoricaine : implication sur la métallogénie de l'uranium. Doctoral dissertation, Université Rennes 1, 308 p.
- Ballouard C., Boulvais P., Poujol M., Gapais D., Yamato P., Tartès R., Cuney M.** (2015) - Tectonic record, magmatic history and hydrothermal alteration in the Hercynian Guérande leucogranite, Armorican Massif, France. *Lithos*, 220–223, 1–22. doi: 10.1016/j.lithos.2015.01.027
- Ballouard C., Poujol M., Boulvais P., Zeh, A.** (2017) - Crustal recycling and juvenile addition during lithospheric wrenching: The Pontivy-Rostrenen magmatic complex, Armorican Massif (France), Variscan belt. *Gondwana Research*, 49, 222–247 doi: 10.1016/j.gr.2017.06.002.
- Barbarin B.** (1999) - A review of the relationships between granitoid types, their origins and their geodynamic environments. *Lithos*, 46, 605–626.
- Bernard-Griffiths J., Peucat J.-J., Sheppard S., Vidal P.** (1985) - Petrogenesis of Hercynian leucogranites from the southern Armorican Massif: contribution of REE and isotopic (Sr, Nd, Pb and O) geochemical data to the study of source rock characteristics and ages. *Earth Planet. Sci. Lett.*, 74, 235–250. doi: 10.1016/0012-821X(85)90024-X
- Bindeman I.** (2008) - Oxygen Isotopes in Mantle and Crustal Magmas as Revealed by Single Crystal Analysis. *Rev. Mineral. Geochem.*, 69, 445–478. doi: 10.2138/rmg.2008.69.12
- Brun J.-P., Gapais D., Cogne J.-P., Ledru P., Vigneresse, J.-L.** (1990) - The Flamanville granite (northwest France): an unequivocal example of a syntectonically expanding pluton. *Geological journal*, 25, 271–286.
- Capdevila R.** (2010) - Les granites varisques du Massif armoricain. *Bull. Société Géologique Minéralogique Bretagne*, 7, 1-52.
- Caroff M., Labry C., Le Gall B., Authemayou C., Grosjean D.-B., Guillong M.** (2015) - Petrogenesis of late-Variscan high-K alkali-calcic granitoids and calc-alkalic lamprophyres: The Aber-Ildut/North-Ouessant complex, Armorican Massif, France. *Lithos*, 238, 140–155. doi: 10.1016/j.lithos.2015.09.025
- Cavosie A.J., Valley J.W., Wilde S.A., E.I.M.F** (2005) - Magmatic d₁₈O in 4400-3900 Ma detrital zircons: A record of the alteration and recycling of crust in the Early Archean. *Earth Planet. Sci. Lett.*, 235, 663–681.
- Chantraine C., Chauvel J-J., Bale P., Denis E., Rabu D.** (1988) - Le Briovérien (Protérozoïque supérieur à terminal) et l'orogenèse cadomienne en Bretagne (France) *Bull. Soc. géol. France*, 5, 815–829.
- Couzinié S., Laurent O., Moyen J.-F., Zeh A., Bouilhol P., Villaros A.** (2016) - Post-collisional magmatism: Crustal growth not identified by zircon Hf–O isotopes. *Earth Planet. Sci. Lett.* 456, 182–195, doi:10.1016/j.epsl.2016.09.033.
- Cuney M., Stussi J.-M., Brouand M., Dautel D., Michard A., Gros Y., Poncet D., Bouton P., Colchen M., Verville J.-P.** (1993) - Géochimie et géochronologie U/Pb des diorites quartziques du Tallud et de Moncoutant: nouveaux arguments pour une extension de la "Ligne Tonalitique Limousine" en Vendée. *C. R. Acad. Sci., Série 2*, 1383–1390.
- Dubois C.** (2014) - Durée de construction, refroidissement et exhumation de l'intrusion composite de Ploumanac'h (Massif Armoricain) : contraintes géochronologiques et thermochronologiques p. 31. Master thesis, Université Rennes 1, 31 p.
- Eiler J.** (2001) - Oxygen isotope variations of basaltic lavas and upper mantle rocks. In: Walley J.W., Cole D.R. (eds) *Reviews in Mineralogy and geochemistry*. The mineralogical society of America, Washington, pp. 319–364
- Euzen T.** (1993) - Pétrogenèse des granites de collision post-épaississement : Le cas des granites crustaux et mantelliques du complexe de Pontivy-Rostrenen (Massif Armoricain, France). Doctoral dissertation, Université Rennes 1, 350 p.
- Faure M., Bé Mézème E., Duguet M., Cartier C., Talbot J-Y.** (2005) - Paleozoic tectonic evolution of medio-europa from the example of the French massif central and massif armoricain. *J. Virtual Expl.*, 19, 26 p.
- Graindor M.-J., Wasserburg G.J.** (1962) - Determinations d'âges absolus dans le Nord du Massif armoricain. *C. R. Séances Hebd. Acad. Sci.*, 3875–3877.

- Hurai V., Paquette J.-L., Huraiová M., Konečný P.** (2010) - U-Th-Pb geochronology of zircon and monazite from syenite and pincinite xenoliths in Pliocene alkali basalts of the intra-Carpathian back-arc basin. *J. Volc. Geotherm. Res.*, 198, 275–287. doi: 10.1016/j.jvolgeores.2010.09.012
- Inglis J.D., Samson S.D., D'Lemos R.S., Hamilton M.** (2004) - U-Pb geochronological constraints on the tectonothermal evolution of the Paleoproterozoic basement of Cadomia, La Hague, NW France. *Precambrian Res.*, 134, 293–315. doi: 10.1016/j.precamres.2004.07.003
- Jackson S.E., Pearson N.J., Griffin W.L., Belousova E.A.** (2004) - The application of laser ablation-inductively coupled plasma-mass spectrometry to in situ U-Pb zircon geochronology. *Chem. Geol.*, 211, 47–69. doi: 10.1016/j.chemgeo.2004.06.017
- Kirkland C. L., Smithies R. H., Taylor R. J. M., Evans N., McDonald B.** (2015) - Zircon Th/U ratios in magmatic environs. *Lithos*, 212, 397–414.
- Le Corre C., Auvray B., Ballèvre M., Robardet M.** (1991) - Le massif Armorican. *Sci. Géol. Bull.*, 44, 31–103.
- Le Gall B., Authemayou C., Ehrhold A., Paquette J.-L., Bussien D., Chazot G., Aouizerat A., Pastol Y.** (2014) - LiDAR offshore structural mapping and U/Pb zircon/monazite dating of Variscan strain in the Leon metamorphic domain, NW Brittany. *Tectonophys.*, 630, 236–250. doi: 10.1016/j.tecto.2014.05.026
- Ludwig K.L.** (2001) - Using Isoplot/EX, v2. 49, a geochronological toolkit for Microsoft Excel. Berkeley Geochronological Centre Spec. Publ.
- Marcoux E., Lebrun E., Bages E.** (2012) - Le skarn à magnétite tardい-hercynien de Diélette (Massif armorican, France). *Géol. France*, 2, 5–25.
- Moyen J.-F., Laurent O., Chelle-Michou C., Couzinié S., Vanderhaeghe O., Zeh A., Villaros A., Gardien V.** (2017) - Collision vs. subduction-related magmatism: Two contrasting ways of granite formation and implications for crustal growth. *Lithos*, 277, 154–177, doi:10.1016/j.lithos.2016.09.018.
- Mullen E.K., Paquette J.-L., Tepper J.H., McCallum I.S.** (2018) - Temporal and spatial evolution of the Northern Cascade Arc magmatism revealed by LA-ICP-MS U-Pb zircon dating. *Canadian J. Earth Sci.*, 55, 443–462. doi: 10.1139/cjes-2017-0167.
- O'Neil J.R., Chappell B.W.** (1977) - Oxygen and hydrogen isotope relations in the Berridale batholith. *J. Geol. Soc.*, 133, 559–571. doi: 10.1144/gsjgs.133.6.0559
- Paquette J.-L., Piro J.-L., Devidal J.-L., Bosse V., Didier A.** (2014) - Sensitivity enhancement in LA-ICP-MS by N2 addition to carrier gas: application to radiometric dating of U-Th-bearing minerals. *Agilent ICP-MS journal*, 58, 4–5.
- Peucat J.-J., Auvray B., Hirbec Y., Calvez J.-Y.** (1984) - Granites et cisaillements hercyniens dans le Nord du Massif Armorican; geochronologie Rb-Sr. *Bull. Soc. Geol. France*, (7), XXVI, 1365–1373. doi: 10.2113/gssgbull.S7-XXVI.6.1365
- Sun S.S., McDonough W.F.** (1989) - Chemical and isotopic systematics of oceanic basalts: Implications for the mantle composition and processes. In: Saunders A.D., Norry M.J. (eds), *Magmatism in the ocean basins*. Geological Society of London, Special Publications, London, pp. 313–345.
- Tartèse R., Poujol M., Ruffet G., Boulvais P., Yamato P., Košler J.** (2011a) - New U-Pb zircon and 40Ar/39Ar muscovite age constraints on the emplacement of the Lizio syn-tectonic granite (Armorican Massif, France). *C. R. Geoscience*, 343, 443–453. doi: 10.1016/j.crte.2011.07.005
- Tartèse R., Ruffet G., Poujol M., Boulvais P., Ireland T.R.** (2011b) - Simultaneous resetting of the muscovite K-Ar and monazite U-Pb geochronometers: a story of fluids: Geochronometers resetting by fluids. *Terra Nova*, 23, 390–398. doi: 10.1111/j.1365-3121.2011.01024.x
- Tera F., Wasserburg G.J.** (1972) - U-Th-Pb systematics in three Apollo 14 basalts and the problem of initial Pb in lunar rocks. *Earth Planet. Sci. Lett.*, 14, 281–304. doi: 10.1016/0012-821X(72)90128-8
- Thiéblemont D., Guerrot C., Simien F., Zammit C.** (2017) - Une compilation des âges radiochronologiques publiés antérieurement à 2016 sur le Massif armorican. Inventaire et mise en forme des données, perspectives pour des acquisitions futures. *Géol. France*, 1, 27–46.
- Van Achterbergh E., Ryan C.G., Jackson S.E., Griffin W.L.** (2001) - Data reduction software for LA-ICP-MS. *Earth Sci. Appl. Min. Assoc Can. Short Course Ser.*, 239–243.
- Vidal P.** (1980) - L'évolution polyorogénique du massif Armorican : apport de la géochronologie et de la géochimie isotopique du strontium. *Mém. Soc. Géol. Mineral. Bretagne*, 21.
- Wiedenbeck M., Allé P., Corfu F., Griffin W.L., Meier M., Oberli F., Quadt A.V., Roddick J.-C., Spiegel W.** (1995) - Three natural zircon standards for U-Th-Pb, Lu-Hf, trace element and REE analyses. *Geostandards and Geoanalytical Research*, 19, 1–23. doi: 10.1111/j.1751-908X.1995.tb00147.x

Appendix 1. Composition of some representative minerals in weight% oxides

Numero	Mineral & Com- ment	SiO ₂	TiO ₂	Al ₂ O ₃	FeO Tot	MnO	MgO	CaO	Na ₂ O	K ₂ O	Cr ₂ O ₃	P ₂ O ₅	F	Cl	Total
4 / 1 .	Pl in perthite	66,95	0,02	19,84	0,03	0,01	0,11	11,38	0,18	0,02	0,01	0,00	0,00	0,00	98,58
10 / 1 .	Pl	63,72	0,04	22,21	0,27	0,06	0,00	3,16	10,14	0,14	0,00	0,06	0,00	0,00	99,81
13 / 1 .	Small Pl	64,50	0,03	22,37	0,17	0,02	0,00	3,05	9,84	0,20	0,04	0,04	0,00	0,00	100,26
33 / 1 .	Pl	65,51	0,01	21,88	0,11	0,00	0,00	2,90	9,84	0,12	0,00	0,00	0,12	0,00	100,49
48 / 1 .	Pl	67,20	0,01	20,92	0,13	0,01	0,03	1,09	10,53	0,26	0,02	0,03	0,00	0,01	100,25
3 / 1 .	perthitic Kfd	63,76	0,00	18,70	0,09	0,00	0,02	0,00	1,57	14,53	0,01	0,00	0,00	0,01	98,73
6 / 1 .	Kfd	65,19	0,02	18,63	0,07	0,00	0,00	0,05	1,67	14,00	0,00	0,00	0,00	0,02	99,65
43 / 1 .	Kfd	65,35	0,00	18,74	0,30	0,00	0,00	0,01	1,19	14,12	0,00	0,00	0,00	0,00	99,72
58 / 1 .	Kfd	65,68	0,03	18,40	0,08	0,00	0,00	0,00	0,82	15,15	0,02	0,03	0,00	0,00	100,24
77 / 1 .	Kfd	65,23	0,01	18,13	0,82	0,02	0,00	0,00	1,03	14,65	0,00	0,00	0,02	0,00	99,91
1 / 1 .	Bt	37,91	4,21	13,22	16,46	0,22	14,27	0,01	0,08	9,38	0,09	0,00	0,24	0,07	96,25
9 / 1 .	Bt	38,05	3,61	13,16	15,93	0,20	14,99	0,01	0,10	9,45	0,03	0,00	0,49	0,06	96,15
35 / 1 .	Bt	38,21	4,58	13,07	16,40	0,18	13,39	0,01	0,01	9,40	0,05	0,06	0,88	0,00	96,24
38 / 1 .	Bt	38,26	4,25	13,44	16,43	0,18	13,64	0,12	0,09	9,08	0,17	0,01	0,81	0,02	96,50
47 / 1 .	Bt	38,93	4,04	13,38	15,99	0,25	14,05	0,02	0,01	9,43	0,04	0,05	0,70	0,00	96,90
15 / 1 .	Amp	50,73	0,47	3,56	11,71	0,34	16,04	12,14	0,89	0,35	0,19	0,05	0,03	0,03	96,95
17 / 1 .	Amp	51,44	0,46	3,20	11,06	0,31	16,38	11,94	0,72	0,27	0,37	0,12	0,07	0,01	96,53
61 / 8 .	Amp	53,19	0,60	3,36	11,51	0,36	15,63	12,06	0,73	0,31	0,00	0,00	0,22	0,00	97,98
61 / 28 .	Amp	45,87	1,60	8,11	14,77	0,32	12,36	11,82	1,60	0,78	0,09	0,05	0,35	0,00	97,74
61 / 33 .	Amp	44,32	1,66	8,45	15,41	0,35	11,81	11,70	1,71	0,98	0,04	0,03	0,34	0,01	96,82

Appendix 2. LA-ICP-MS zircon U-Th-Pb isotope data for the Flamanville granodiorite

<i>Flamanville Granodiorite</i>		Spot	Pb (ppm)	Th (ppm)	U (ppm)	Th/U	$^{207}\text{Pb}/^{235}\text{U}$	$^{207}\text{Pb}/^{238}\text{U}$	$^{206}\text{Pb}/^{235}\text{U}$	$^{206}\text{Pb}/^{238}\text{U}$	$^{206}\text{Pb}/^{238}\text{U}$	Age (Ma)	$^{2\sigma}$ error	$^{206}\text{Pb}/^{238}\text{U}$	$^{206}\text{Pb}/^{238}\text{U}$	
A01 c	74	743	1342	0,55	0,3755	0,0116	0,05036	0,00141	319,8				8,6			
A02 c	66	544	1231	0,44	0,3798	0,0154	0,05064	0,00144	318,4				8,8			
A03 c	42	400	771	0,52	0,3695	0,0117	0,05057	0,00138	318,0				8,5			
A04 c	50	530	896	0,59	0,3836	0,0120	0,05146	0,00141	323,5				8,7			
A06 c	95	1013	1714	0,59	0,3899	0,0123	0,05056	0,00138	317,9				8,5			
A08 c	62	581	1157	0,50	0,3678	0,0114	0,05073	0,00138	319,0				8,6			
B01 c	18	105	345	0,31	0,3742	0,0130	0,05126	0,00141	322,3				8,7			
B02 c	91	803	1640	0,49	0,4296	0,0140	0,05089	0,00141	320,0				8,6			
B03 c	83	876	1494	0,59	0,3674	0,0124	0,05066	0,00141	318,6				8,6			
B05 c	81	614	1503	0,41	0,3932	0,0140	0,05139	0,00144	323,1				8,8			
B06 c	82	746	1489	0,50	0,4144	0,0125	0,05074	0,00138	319,1				8,5			
B08 c	540	12796	7469	1,71	0,3657	0,0107	0,05030	0,00138	316,4				8,4			
C01 c	47	400	897	0,45	0,3703	0,0122	0,05058	0,00138	318,1				8,6			
C02 c	78	697	1427	0,49	0,4296	0,0139	0,05053	0,00138	317,8				8,6			
C04 c	32	269	597	0,45	0,4319	0,0140	0,05028	0,00138	316,2				8,5			
C05 r	37	238	699	0,34	0,3793	0,0155	0,05064	0,00141	318,5				8,7			
C06 r	93	721	1732	0,42	0,3969	0,0121	0,04998	0,00138	314,4				8,4			
C07 c	36	224	661	0,34	0,4332	0,0138	0,05102	0,00141	320,8				8,6			
C08 c	74	691	1232	0,56	0,5754	0,0181	0,05063	0,00138	318,4				8,6			
D02 c	67	578	1229	0,47	0,3731	0,0116	0,05071	0,00138	318,9				8,5			
D03 c	77	808	1339	0,60	0,4190	0,0130	0,04992	0,00138	314,0				8,4			
D05 c	40	397	692	0,57	0,4744	0,0151	0,05043	0,00138	317,2				8,5			
D06 r	52	492	946	0,52	0,3893	0,0123	0,05077	0,00138	319,3				8,6			
D07 r	71	670	1233	0,54	0,5057	0,0156	0,05058	0,00138	318,1				8,5			
E01 c	78	611	1332	0,46	0,6014	0,0190	0,05050	0,00138	317,6				8,5			
E02 c	40	361	763	0,47	0,3786	0,0130	0,04930	0,00135	310,2				8,4			
E03 r	66	677	1063	0,64	0,6335	0,0206	0,05043	0,00138	317,2				8,6			
E04 r	77	756	1340	0,56	0,4990	0,0158	0,05028	0,00138	316,2				8,5			
E06 r	39	362	723	0,50	0,3662	0,0140	0,05023	0,00141	316,0				8,6			
E07 c	50	467	910	0,51	0,4030	0,0148	0,05064	0,00141	318,4				8,6			
E08 r	51	435	948	0,46	0,3829	0,0142	0,05058	0,00141	318,1				8,6			

Appendix 3. LA-ICP-MS zircon U-Th-Pb isotope data for the anse du Cul-Rond gneiss.

Anse du cul-rond Gneiss		Spot	Pb ppm	Th ppm	U ppm	Th/U	$^{207}\text{Pb}/^{235}\text{U}$	$^{207}\text{Pb}/^{238}\text{U}$	$^{206}\text{Pb}/^{238}\text{U}$	$^{206}\text{Pb}/^{207}\text{Pb}$	$^{207}\text{Pb}/^{206}\text{Pt}$	$^{207}\text{Pb}/^{206}\text{Pb}$	Age (Ma)	2σ error
A01 c	71	50	191	0,26	6,196	0,183	0,35587	0,0097	2033	57				
A02 c	62	19	168	0,11	6,454	0,189	0,3704	0,0100	2048	57				
A03 c	76	55	195	0,28	6,425	0,188	0,3714	0,0100	2035	57				
A04 r	144	42	389	0,11	6,403	0,185	0,3701	0,0100	2035	56				
A05 c	46	15	125	0,12	6,204	0,185	0,3607	0,0098	2025	58				
A06 c	107	28	313	0,09	5,852	0,169	0,3434	0,0092	2008	56				
A07 c	97	107	238	0,45	6,469	0,187	0,3704	0,0100	2052	56				
B01 c	76	51	195	0,26	6,529	0,188	0,3738	0,0101	2052	56				
B02 c	68	39	177	0,22	6,416	0,184	0,3706	0,0100	2037	56				
B03 c	66	31	174	0,18	6,501	0,187	0,3730	0,0101	2048	56				
B04 c	125	90	333	0,27	6,208	0,177	0,3591	0,0096	2034	56				
B05 c	23	2	283	0,007	0,728	0,032	0,0882	0,0025	597	100				
B06 c	47	23	122	0,19	6,526	0,189	0,3740	0,0101	2050	56				
B08 c	57	33	150	0,22	6,307	0,182	0,3623	0,0098	2046	56				
C01 c	45	20	119	0,17	6,361	0,186	0,3658	0,0099	2045	57				
C03 c	130	59	340	0,17	6,490	0,183	0,3726	0,0100	2047	55				
C04 c	77	27	203	0,13	6,498	0,185	0,3721	0,0100	2052	56				
C05 c	107	23	287	0,08	6,529	0,184	0,3736	0,0100	2053	55				
C06 c	77	21	207	0,10	6,491	0,184	0,3725	0,0100	2048	56				
C07 c	106	23	293	0,08	6,256	0,177	0,3626	0,0097	2031	55				
C08 c	46	38	113	0,33	6,569	0,190	0,3750	0,0101	2057	56				
D01 r	155	33	425	0,08	6,377	0,191	0,3685	0,0100	2036	58				
D01 c	60	34	161	0,21	6,290	0,190	0,3648	0,0099	2029	58				
D02 c	141	66	383	0,17	6,246	0,185	0,3612	0,0098	2034	57				
D03 c	86	45	233	0,19	6,264	0,186	0,3632	0,0098	2030	58				
D04 c	106	79	276	0,29	6,358	0,189	0,3653	0,0099	2046	58				
D05 c	100	43	264	0,16	6,423	0,190	0,3717	0,0100	2033	57				
D06 c	41	17	108	0,16	6,338	0,192	0,3706	0,0101	2015	59				
D08 c	41	34	108	0,31	6,361	0,195	0,3629	0,0099	2058	59				